Evolution of native point defects in ZnO bulk probed by positron annihilation spectroscopy

2009 Chinese Phys. B 18 2072

(http://iopscience.iop.org/1674-1056/18/5/058)

Vol 18 No 5, May 2009
1674-1056/2009/18(05)/2072-06

Chinese Physics B

Evolution of native point defects in ZnO bulk probed by positron annihilation spectroscopy

Peng Cheng-Xiao(彭成晓)[a)†], Wang Ke-Fan(王科范)[a)], Zhang Yang(张 杨)[a)], Guo Feng-Li(郭凤丽)[a)], Weng Hui-Min(翁惠民)[b)], and Ye Bang-Jiao(叶邦角)[b)]

[a)] *Physics and Electronics School, Henan University, Kaifeng* 475004, *China*
[b)] *Modern Physics Department, University of Science and Technology of China, Hefei* 230026, *China*

(Received 17 September 2008; revised manuscript received 24 October 2008)

This paper studies the evolution of native point defects with temperature in ZnO single crystals by positron lifetime and coincidence Doppler broadening (CDB) spectroscopy, combined with the calculated results of positron lifetime and electron momentum distribution. The calculated and experimental results of the positron lifetime in ZnO bulk ensure the presence of zinc monovacancy, and zinc monovacancy concentration begins to decrease above 600 °C annealing treatment. CDB is an effective method to distinguish the elemental species, here we combine this technique with calculated electron momentum distribution to determine the oxygen vacancies, which do not trap positrons due to their positive charge. The CDB spectra show that oxygen vacancies do not appear until 600 °C annealing treatment, and increase with the increase of annealing temperature. This study supports the idea that green luminescence has a close relation with oxygen vacancies.

Keywords: positron annihilation, ZnO native defects
PACC: 7870B, 7165

1. Introduction

The semiconductor zinc oxide (ZnO), whose many excellent properties and success in producing large-area single crystals make it a promising material in optoelectronic devices, has recently attracted a great deal of attention. The combination of a large direct band gap of 3.37 eV and 60 meV exciton binding energy at room temperature makes ZnO an important application to the ultraviolet light emission source.[1,2] In addition, as compared to the situation in Si and GaAs, ZnO is quite resistant to displacement damage. This fact suggests that it could be used in the space environment where particle irradiation is strong.[3]

Lots of experiments indicate that point defects in ZnO play a significant role in its electrical and optical performance.[4,5] Undoped ZnO usually exhibits n-type conductivity, and the reason accounting for the prevalence of n-type conductivity in undoped ZnO is suggested as those donor defects such as Zn interstitials (Zn_i), O vacancies (V_O)[6,7] and hydrogen background impurities.[8−10] Nevertheless most arguments have been based on circumstantial evidence, in the absence of unambiguous experimental observation. Besides the effect of native point defects on electrical properties, they also lead to a green luminescence band. But up to date identification of the recombination centres and mechanisms responsible for many of the luminescence properties are still a matter of controversy. Different origins of the green emissions have been proposed, such as Zn_i,[11] V_O,[12−14] O_{Zn},[15] V_{Zn},[16,17] and Cu-related defects.[18,19] So it is essential to exactly characterize and distinguish these defects, which could make us further understand the mechanism between defect and host.

Positron annihilation spectroscopy (PAS) is a powerful and sensitive technique to detect open-volume defects in metals, semiconductors, polymers and nanomaterials.[20,21] When a positron is implanted into condensed matter, it annihilates with an electron mainly into 511 keV γ quanta. The momentum of the positron–electron pair causes a Doppler shift in the energy of the annihilating photons. In the material containing defects, a freely diffusing positron can be readily localized or trapped at open-volume defects as a result of the missing positive-ion cores at these defects. The trapping will lead to a narrowing of the momentum distribution of the positron–electron pair and the annihilating photons, which is reflected in the shift of Doppler broadening spec-

†E-mail: pengcx@mail.ustc.edu.cn

troscopy. In conventional one detector Doppler broadening experiments, this technique used to be restricted to probe distribution of lower momentum regions of the electrons due to bad peak to ground ratio. Recently the background suppressed coincidence Doppler broadening (CDB) technique was developed, whose peak to ground ratio was improved by two orders of magnitude, thus the momentum distribution of core electrons could be measured. While core electrons strongly reflect the elemental information, CDB could be used to discriminate the element species.

2. Experiment

ZnO single crystals (10 cm × 10 cm × 0.5 cm) were supplied by the Hefei Kejing Materials Technology Corporation Limited. These samples were hydrothermally grown. They were nominally undoped and annealed isochronally at 200, 400, 600, 800 and 1000 °C for 30 min in nitrogen gas, respectively, then cooled slowly to room temperature.

The positron lifetimes in as-grown ZnO and in the ZnO annealing treatment were measured by a fast–fast coincidence positron lifetime system with the resolution 210 ps. For each positron lifetime spectrum about 10^6 counts were recorded.

The CDB setup is constructed by two high purity Ge detectors placed oppositely with the distance of 30 cm. The peak to background is about 10^5 and effective count rate is about 80 cps.[22] The Na source and two identical samples form a 'sandwich' structure. For each temperature $\sim 10^7$ coincidence counts were recorded.

The positron lifetime and electron momentum distribution were calculated by two-component density functional theory, the electron density and the Coulomb potential non-self-consistently are archived by using the atomic superposition method.[22] Here we used the Doppler software package to calculate the positron lifetime and momentum distribution, which was developed by the positron group at Helsinki University.[23]

3. Results and discussion

The positron lifetimes calculated are 178 ps, 181 ps, and 235 ps in perfect ZnO bulk single crystals, ZnO containing oxygen vacancies and zinc vacancies, respectively. These results are consistent with Tuomisto's results.[24] In Brauer's report, the lifetimes are 176 ps and 178 ps in ZnO bulk and in ZnO containing oxygen vacancies by atomic superposition with a gradient correction (ATSUP-GC).[25] Our results are also close to Brauer's results except the positron lifetime at zinc vacancies. Our positron lifetime for zinc vacancy is shorter than Brauer's result, because no relaxation has been considered in our work. The structure relaxation has more importance for positron trapping centres (here zinc vacancies), while structure relaxation is less important to bulk and oxygen vacancies.

The measured positron lifetime spectra for ZnO samples were decomposed into three lifetime components using PATFIT[26] and LT 9.0.[27] For all samples τ_1, τ_2 and its intensity are listed in Table 1. For all samples τ_3 are more than 1.5 ns with about 2% low intensity, which are considered as positron annihilation in the Kapton film sealing the positron source,[28] therefore τ_3 could be ignored. The positron bulk lifetime τ_b is deduced according to the equation $\tau_b = (I_1 + I_2)/(I_1/\tau_1 + I_2/\tau_2)$. The τ_b varies from 160 to 174. In terms of calculated results and Tuomisto's report,[24] 170 ps is considered as the positron bulk lifetime in a perfect ZnO crystal.

Table 1. The measured positron lifetimes for as-grown annealed at various temperatures.

sample	τ_1/ps	τ_2/ps	I_2/%	τ_{av}/ps
as grown	109(±2)	232(±4)	67.6(±0.7)	194(±3)
200 °C	94(±4)	236(±5)	70.2(±1.6)	196(±5)
400 °C	90(±5)	242(±2)	69.0(±0.9)	196(±3)
600 °C	94(±3)	244(±1)	68.1(±0.5)	198(±2)
800 °C	101(±2)	245(±4)	61.1(±0.7)	191(±3)
1000 °C	133(±5)	237(±2)	52.9(±0.6)	189(±3)

For as-grown ZnO and other samples, τ_2 is about 235 ps, τ_2 could represent the defect size, so it can be determined by zinc vacancies in ZnO bulk according to the calculated results. In addition, the identification defect type also could use the ratio of τ_d/τ_b, and here this value is about 1.36–1.44, which corresponds to positron lifetime at monovacancies. The ratio is in agreement with Brunner's[29] and Tuomisto's reports[24] (their ratios are 1.30 and 1.35 respectively).

The τ_{av} could accurately reflect the defect variation, which coincides with the centre of mass of the spectrum, and it has the smallest experimental error. The τ_{av} could be calculated by the equation $\tau_{av} = (I_1\tau_1 + I_2\tau_2)/(I_1 + I_2)$. The τ_{av} almost remains a constant 196 ps below 600 °C annealing treatment, but this value sharply decreases to 191 ps after 800 °C annealing. In response to the positron average lifetime, τ_b and τ_d, we can utilize the following expression to roughly estimate the defect concentration in ZnO

$$k = \mu C = \frac{(\tau_{av} - \tau_b)}{\tau_b(\tau_d - \tau_{av})},$$

where κ is the trapping rate, C is the defect concentration and μ the positron trapping coefficient. In the ZnO bulk $\mu = 3\times10^{15}\,s^{-1}$,[24] here we use this number to evaluate the defect concentration. The dependence of zinc vacancy concentration on annealing temperature is shown in Fig.1. Zinc vacancy concentration dramatically decreases above 600 °C annealing treatment.

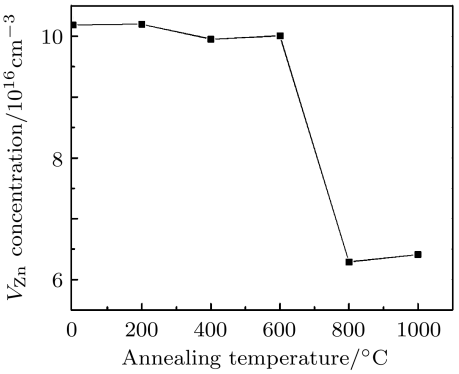

Fig.1. The dependence of zinc vacancy concentration on annealing temperature.

On the basis of the variation of positron lifetimes at defects, one can exclude the presence of the zinc vacancy and hydrogen cluster, as well as zinc vacancy and oxygen cluster. Although hydrogen is usually in hydrothermally grown ZnO, here the complex of zinc vacancy and hydrogen is impossible. If complexes of zinc vacancy and hydrogen are present, the hydrogen becomes unstable at high temperature and desorption of the hydrogen occurs at 500–700 °C annealing.[30,31] This will make the open volume of the complex larger and τ_d will sharply increase, such as from 160 ps to 200 ps corresponding to V_{Zn} + 4H and V_{Zn} + H.[32] But our results show that the positron lifetimes around defects decrease with the increase of annealing temperature. A similar analysis could be applied to the clusters formed by zinc vacancy and oxygen atom. Oxygen atoms usually escape from the ZnO after the annealing treatment, so the clusters will become larger and the positron lifetime increases. This change of positron lifetime is opposite to our experimental results.

The electron momentum distributions were calculated for the ZnO bulk state, the oxygen vacancy and the zinc vacancy, respectively. Figure 2 shows the momentum distribution of the main individual shells of Zn and O atoms. It can be seen that a positron predominantly annihilates with a Zn 4s electron in the range of (0–4) $\times10^{-3}m_0c$, while an oxygen 2p electron prevails from 4 to $9\times10^{-3}m_0c$, and in higher momentum regions positron annihilation occurs with a Zn 3d electron overwhelmingly.

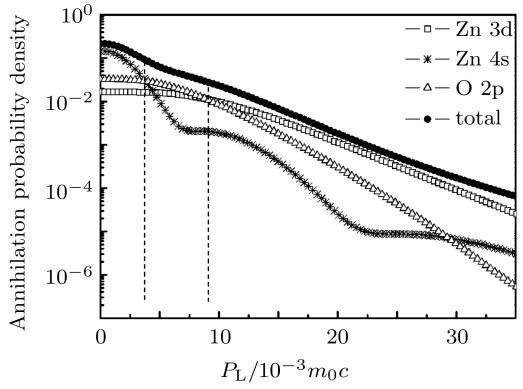

Fig.2. The positron annihilation probability with electrons at different shells of Zn and O atoms according to calculated results.

Figure 3 shows the ratio curves of the ZnO defect state with respect to the ZnO bulk state. In lower regions the ratio curve drops for ZnO containing an oxygen vacancy and a dip locates at about $6\times10^{-3}m_0c$, then extends near the 2.54 cm higher momentum region. However, as for ZnO containing a Zn vacancy it is an opposite trend. Therefore different defects due to missing atoms play an important role in the shape of the ratio curve. It is known that zinc vacancies in

ZnO bulk show negative charges, while oxygen vacancies are positively charged. So zinc vacancies could effectively trap positrons, while oxygen vacancies could not. In the region of 4 to $9 \times 10^{-3} m_0 c$ the positron mostly annihilates with an oxygen 2p electron, which reveals the positron annihilation with the oxygen sublattice in ZnO.

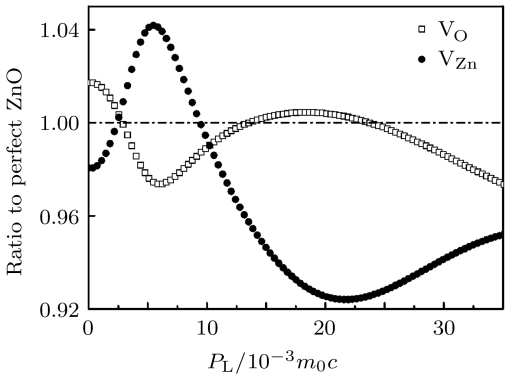

Fig.3. The ratio curves of imperfect ZnO in contrast to perfect ZnO.

Figure 4 shows ratio curves for the samples after annealing treatment to as-grown ZnO. It can be seen that the ratio curve almost equals 1 in contrast to as-grown ZnO, when the annealing temperature is 600 °C. With the increase of temperature, the curves ascend in the range of $P_L < 4 \times 10^{-3} m_0 c$, while they decrease from $4 \times 10^{-3} m_0 c$ to $9 \times 10^{-3} m_0 c$.

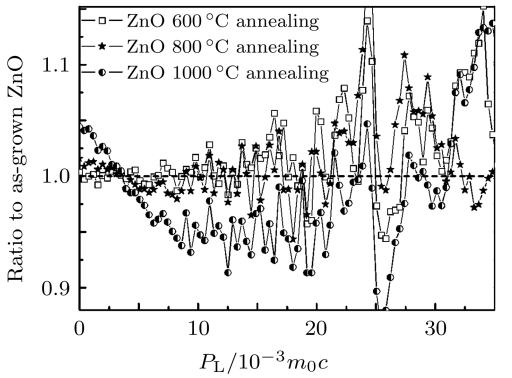

Fig.4. The ratio curves of annealing ZnO with respect to as-grown ZnO.

In order to clearly show the change in CDB spectra, two parameters are defined, R_{Zn} and R_O. The R_{Zn} is the ratio of the integral of ray counts from 0 to $4 \times 10^{-3} m_0 c$ to the total counts of spectrum, and this lower momentum region represents Zn 4s electrons annihilating with positrons. Similarly, R_O is the total counts in the range of $(4–9) \times 10^{-3} m_0 c$ with respect to the total counts of the spectrum, which is a good measurement of the fraction of positrons annihilating with the oxygen 2p electrons. Figure 5 reveals the variation of R_{Zn} and R_O with the annealing temperature. When the temperature is below 600 °C, R_{Zn} and R_O almost remain at 0.702 and 0.274, respectively. R_{Zn} increases, while R_O decreases at higher temperatures. It is considered that zinc vacancy concentration does not vary at lower temperatures, and when the temperature is above 600 °C, ZnO decomposition happens. The decomposability process could be depicted by the following formula:[33]

$$\mathrm{ZnO} \rightarrow \mathrm{Zn_{Zn}} + \mathrm{V_O} + \frac{1}{2}\mathrm{O_2}.$$

When ZnO decomposability occurs, one oxygen atom escapes from the host, at the same time, one zinc atom is left behind. With the increase of annealing temperature, the ZnO decomposability is enhanced, so more zinc atoms are left behind in the ZnO sample. When the annealing temperature is high enough, some zinc atoms could move, and recombination between zinc atoms and zinc vacancies can occur. Some zinc vacancies disappear, and the possibility of positron annihilation with Zn 4s electrons increases. On the other hand, R_O decreases with the increase of temperature, which means that the possibility of positron annihilation with O 2p electrons falls due to oxygen evaporation at elevated temperature.

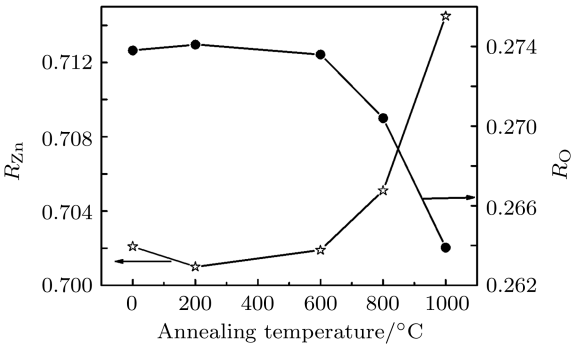

Fig.5. The variation of R_{Zn} and R_O with annealing temperature.

In order to understand the influence of native defects in ZnO on optical properties, the photoluminescence (PL) spectra were measured. Figure 6 shows PL spectra, which were measured at room temperature after annealing at different temperatures. It indicates that green peaks centred between 480 and 540 nm (2.30–2.56 eV) do not appear until annealing above 600 °C. This green luminescence has been attributed to many defects, such as Cu impurities, a zinc

vacancy, interstitial zinc (Zn_i), oxygen antisite (O_{Zn}), and oxygen vacancy. For the copper impurity source not all ZnO samples contain copper, and it is hard to explain the variation of green luminescence intensity in this work. As for interstitial zinc, its migration barrier is as low as 0.57 eV, so it is unlikely to be stable.[17] If interstitial zinc is responsible for the visible emission, one is unlikely to observe the zinc vacancy by positron annihilation spectra. Some studies suggest that a zinc vacancy could give rise to green luminescence, but Chen's report clearly points out that zinc vacancies are not related to visible emission according to cathodoluminescence measurements.[31] Figure 7 shows the variation of positron average lifetime and green luminescence intensity with annealing temperature, here the counts at 510 nm act as the intensity of green luminescence. If the green luminescence is ascribed to a zinc vacancy, green luminescence intensity enhancement means the increase of zinc vacancy concentration, which is contrary to the variation of positron lifetime.

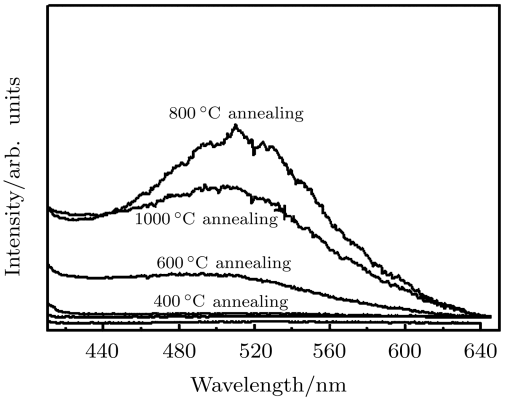

Fig.6. Room temperature photoluminescence spectra of ZnO samples heat treated at various temperatures.

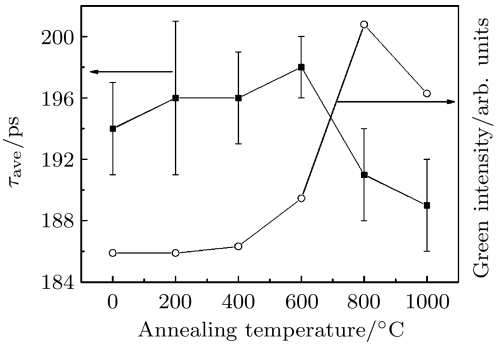

Fig.7. The variation of the positron average lifetime and green luminescence intensity with annealing temperature.

Therefore this work does not support the suggestion of a zinc vacancy being responsible for the green luminescence. According to the positron lifetime and CDB spectra, an oxygen vacancy is the most possible origin of the green luminescence. ZnO decomposition above 600 °C annealing leads to oxygen atoms escaping from ZnO bulk, so an oxygen vacancy appears. The oxygen vacancy increases after higher temperature treatment, which is consistent with the CDB spectra.

4. Summary

In conclusion, the evolution of oxygen and zinc vacancies with annealing temperature has been observed by positron annihilation spectra and PL spectra, and these results are in agreement with theoretical calculations. Zinc vacancies decrease and oxygen vacancies increase due to ZnO decomposition after 600 °C annealing.

References

[1] Sundqvist P A, Zhao Q X and Willander M 2003 *Phys. Rev.* B **68** 155334

[2] Özgü Ü, Alivov Ya I, Liu C, Teke A, Reshchikov M A, Doğn S, Avrutin V, Cho S J and Morkoc H 2005 *J. Appl. Phys.* **98** 041301

[3] Look D C, Reynolds D C, Fang Z Q, Hemsky J W, Sizelove J R and Jones R L 1999 *Mater. Sci. and Eng.* **66** 30

[4] Jin B J, Bae S H, Lee S Y and Im S 2003 *Mater. Sci. and Eng.* B **71** 301

[5] Look D C, Coskun C, Claflin B and Farlow G C 2003 *Physica* B **340–342** 32

[6] Look D C, Hemsky J W and Sizelove J R 1999 *Phys. Rev. Lett.* **82** 2552

[7] Look D C, Farlow G C, Reunchan P, Limpijumnong S, Zhang S B and Nordlund K 2005 *Phys. Rev. Lett.* **95** 225502

[8] van de Walle C G 2000 *Phys. Rev. Lett.* **85** 1012

[9] Hofmann D M, Hofstaetter A, Leiter F, Zhou H, Henecker F, Meyer B K, Orlinskii S B, Schmidt J and Baranov P G 2002 *Phys. Rev. Lett.* **88** 045504

[10] Selim F A, Weber M H, Solodovnikov D and Lynn K G 2007 *Phys. Rev. Lett.* **99** 085502

[11] Jeong S H, Kim B S and Lee T B 2003 *Appl. Phys. Lett.* **82** 2625

[12] Vanheusden K, Seager C H, Warren W L, Tallant D R and Voigt J A 1996 *Appl. Phys. Lett.* **68** 403

[13] Kang J S, Kang H S, Pang S S, Shim E S and Lee S Y 2003 *Thin Solid Films* **443** 5

[14] Kang H S, Kang J S, Kim J W and Lee S Y 2004 *J. Appl. Phys.* **95** 1246
[15] Lin B X, Fu Z X and Jia Y B 2001 *Appl. Phys. Lett.* **79** 943
[16] Zhao Q X, Klason P, Willander M, Zhong H M, Lu W and Yang J H 2005 *Appl. Phys. Lett.* **87** 211912
[17] Janotti A and van de Walle C G 2007 *Phys. Rev.* B **76** 165202
[18] Garces N Y, Wang L, Bai L, Giles N C, Halliburton L E and Cantwell G 2002 *Appl. Phys. Lett.* **81** 622
[19] Alivov Ya I, Chukichev M V and Nikitenko V A 2004 *Semiconductors* **38** 34
[20] Brandt W and Dupasquicr A 1983 *Positron Solid State Physics* (Amsterdam: North-Holland)
[21] Krause-Rehberg R and Leipner H S 1999 *Positron Annihilation in Semiconductors* (Berlin: Springer)
[22] Hakala M, Puska M J and Nieminen R M 1998 *Phys. Rev.* B **57** 7621
[23] Makkonen I, Hakala M and Puska M J 2006 *Physica* B **376–377** 971
[24] Tuomisto F, Ranki V, Saarinen K and Look D C 2003 *Phys. Rev. Lett.* **91** 205502
[25] Brauer G, Anwand W, Skorupa W, Kuriplach J, Melikhova O and Moisson C 2006 *Phys. Rev.* B **74** 045208
[26] Kirkegaard P, Eldrup M, Mogensen O E and Pedersen N J 1981 *Comput. Phys. Commun.* **23** 307
[27] Kansy J 1996 *Nucl. Instrum. Mech.* A **374** 235
[28] Hernández-Fenollosa M A, Damonte L C and Marí B 2005 *Superlattices and Microstructures* **38** 336
[29] Brunner S, Puff W, Balogh A G and Mascher P 2001 *Mater. Sci. Forum* **363–365** 141
[30] Look D C, Jones R L, Sizelove J R, Garces N Y, Giles N C and Halliburton L E 2003 *Phys. Stat. Sol.* (a) **195** 171
[31] Chen Z Q, Wang S J, Maekawa M, Kawasuso A, Naramoto H, Yuan X L and Sekiguchi T 2007 *Phys. Rev.* B **75** 245206
[32] Brauer G, Kuriplach J, Cizek J, Anwand W, Melikhova O, Prochazka I and Skorupa W 2007 *Vacuum* **81** 1314
[33] Chen Z Q, Yamamoto S, Maekawa M, Kawasuso A, Yuan X L and Sekiguchi T 2003 *J. Appl. Phys.* **94** 4807